Geophysical Journal International

Geophys. J. Int. (2023) **234,** 1870–1884 https://doi.org/10.1093/gji/ggad172
Advance Access publication 2023 April 24
GJI Seismology

On the time-stability of resonance frequencies in deep basins

Giovanni Lattanzi, Silvia Castellaro and Miriana Di Donato

Dipartimento di Fisica e Astronomia – Alma Mater Studiorum Università di Bologna, viale C. B. Pichat 8, 40126 *Bologna, Italy.*
E-mail: giovanni.lattanzi90@gmail.com

Accepted 2023 April 12. Received 2023 March 14; in original form 2022 September 15

SUMMARY

Determining the resonance frequencies of sediment-filled basins is important in seismic site effects assessment and to infer information about the geometrical and mechanical properties of the basins. Being intrinsic properties of elastic bodies, resonance frequencies are not expected to change over time, at least in the short term and under small excitations, in this type of basins. By analysing multi-annual time-series at some seismic stations located on markedly alpine and subalpine 2-D basins, we first state under what type of exciting function (ambient noise) these resonances can be identified and with what uncertainty. The analysis will reveal a clear annual and daily oscillation of the resonance frequencies, increasing in the summertime and at daytime (i.e. directly correlated with temperature). We attempt to provide different explanations to this not yet so systematically documented experimental evidence. A clear and unique answer is yet to come.

Key words: Fourier analysis; Wave propagation; Sedimentary basin processes; Basin resonance.

1 INTRODUCTION

2-D resonances have long been acknowledged in alpine sediment-filed valleys (Roten *et al.* 2006; Gúeguen *et al.* 2007; Le Roux *et al.* 2012; Ermert *et al.* 2014; Sgattoni & Castellaro 2020). Experimental surveys to detect them rely on arrays of synchronized stations, providing the modal shapes along basin cross-sections (Ermert *et al.* 2014), on the surface-to-bedrock spectral ratios (Roten *et al.* 2006) or simply on asynchronous single station measurements (Sgattoni & Castellaro 2020).

These natural vibration modes are of interest both to predict the seismic response of the sediment-filled basins (e.g. Lebrun *et al.* 2002; Di Giulio *et al.* 2016; Khanbabazadeh *et al.* 2019) and to get information on their geometrical and mechanical properties (Suzuki *et al.* 2021; Castellaro & Musinu 2023). White noise excitations would allow for an immediate identification of these natural modes, while this may not be the case under non-white excitation, which is the rule with ambient noise (Peterson 1993). Non-white excitations can affect the amplitude of the ground motion at different frequencies and can potentially mask some resonances, enhancing other vibration frequencies. Determining under what excitation the natural modes can be identified and the uncertainty in their determination is therefore important. Being intrinsic properties of elastic bodies, the natural modes of deep sediment-filled basins are expected not to significantly vary over time, in the short term and clearly excluding the presence of non-linear phenomena (e.g. earthquakes).

In this paper, we study the identifiability and time-stability of the modal frequencies of several fluvial/glacial sedimentary basins. This study will reveal an interesting time-dependent property of these natural vibration modes, not yet fully reported on individual spectra.

2 THE SELECTED CASES

Considering a cross-section of an idealized fluvial/glacial valley/basin, the main natural modes have the shapes given in Fig. 1 and extensively discussed in Castellaro & Musinu (2023). Following their notation, we name longitudinal (L) the modes causing displacement along the longitudinal axis, transverse (T) the modes with a mostly transverse displacement and vertical (V) those with a main vertical displacement. Transverse modes necessarily imply some vertical displacement (Fig. 1) but this is much smaller than the transverse one.

We restrict the analysis to basins having fundamental natural frequencies larger than 0.2 Hz. Below this value, the influence of the oceanic-tidal effect becomes dominant over stratigraphic resonances in microtremor spectra (Longuet-Higgins 1950; Haubrich *et al.* 1963). Also, we focus on basins with aspect ratios (maximum height divided by half-width, h/w in Fig. 1) between 0.2 and 0.5, that is on markedly 2-D conditions (assuming the third dimension as 'infinite') and on basins where permanent seismic stations are present on the sediment filling.

Last, we select only basins whose dynamic properties (natural frequencies) have been previously assessed by other authors by

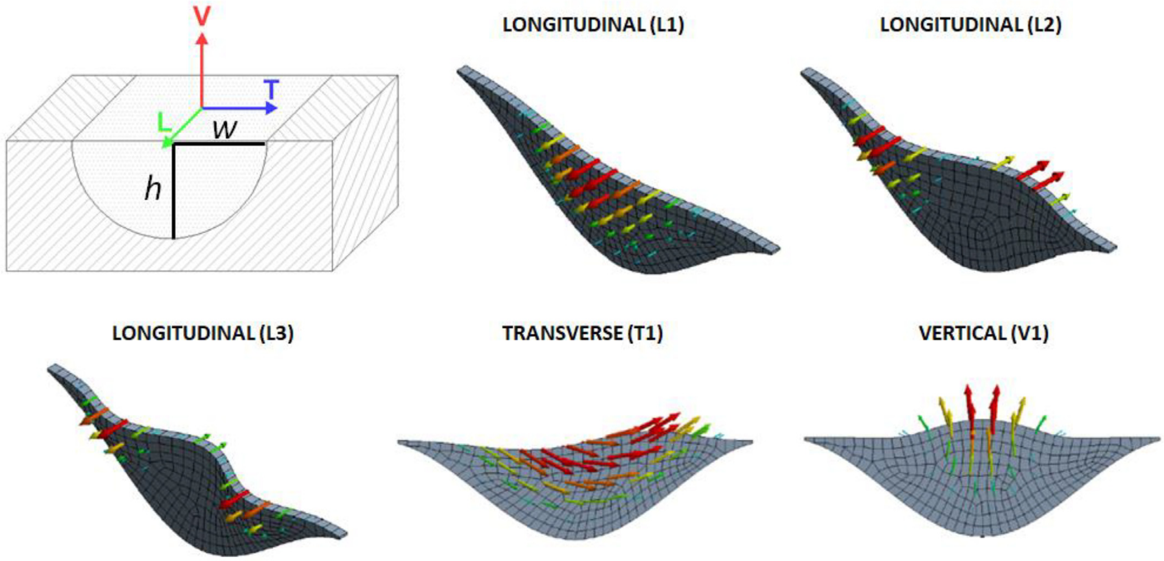

Figure 1. Top left-hand panel: principal directions of motion of an idealized basin with aspect ratio h/w. Other panels: longitudinal ($\boldsymbol{L}_1$, $\boldsymbol{L}_2$, $\boldsymbol{L}_3$), transverse ($\boldsymbol{T}_1$) and vertical ($\boldsymbol{V}_1$) mode shapes for a cross-section of the sediment-filled basin. Red colour indicates the maximum displacement and arrows the direction of motion.

	SEFS	SIOO	OGFO	BOSI	GARG
Location	Reuss valley (Switzerland)	Rhône valley (Switzerland)	Grenoble basin (France)	Bolzano basin (Italy)	Bolzano-Merano valley (Italy)
References	Hobiger & Fäh 2020	Ermert et al. 2014	Delépine & Semblat 2012	Sgattoni & Castellaro 2020	Castellaro & Musinu 2023
Eigen-frequencies	L1: 0.552 Hz T1: 0.696 Hz V1: 0.979 Hz	L1: 0.457 Hz T1: 0.523 Hz V1: 0.793 Hz	L1: 0.320 Hz T1: 0.352 Hz	L1: 0.330 Hz T1: 0.389 Hz	L1: 0.283 Hz T1: 0.328 Hz L2: 0.368 Hz L3: 0.436 Hz
Mean aspect ratio	0.50	0.37	0.22	0.40	0.30
Valley morphology	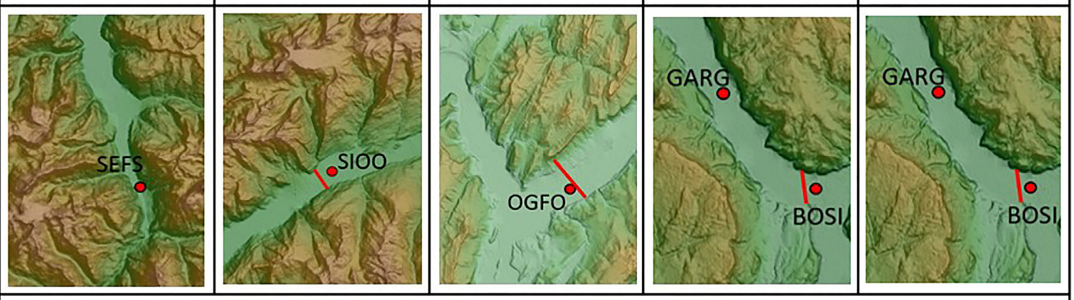				
Valley section	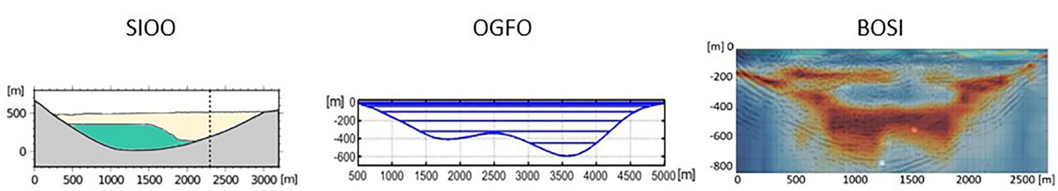				

Figure 2. Main features of the studied basins. The modal frequency and basin shape information come from the extensive field surveys of the authors listed in the References field. No section is available for SEFS and GARG.

means of extensive experimental geophysical surveys. The selected cases are: (1) Reuss valley (Switzerland), (2) Rhône valley (Switzerland), (3) Grenoble basin (France), (4) Bolzano basin (Italy) and (5) Bolzano-Merano valley (Italy).

The main geometrical and vibration properties of each basin are summarized in Fig. 2. Details about the seismic/accelerometric stations present at each selected site [respectively, (1) CH.SEFS, (2) CH.SIOO, (3) RA.OGFO, (4) IT.BOSI and (5) GARG] are given

Table 1. Main features of the seismic and accelerometric instrumental chains installed at the analysed seismic stations. Coordinates are given in WGS84, decimal degrees. The analysed stations belong respectively to CH, National Seismic Networks of Switzerland; RA, RESIF RAP Accelerometric permanent network; S, Sudtirol Network, Italy. The frequency range indicated for accelerometers, which are low-pass sensors, is just nominal.

Station network	CH	CH	RA	SI	–
Station name	SEFS	SIOO	OGFO	BOSI	GARG
Latitude	46.81869°N	46.23280°N	45.20874°N	46.49520°N	46.58455°N
Longitude	8.64850°E	7.38320°E	5.82101°E	11.31850°E	11.19314°E
Time interval	Jul 2017–Jan 2022	Jan 2017–Jan 2022	Jan 2017–Jan 2022	Jan 2017–Jan 2022	Feb 2021–May 2022
Sensor	Kinemetrics EpiSensor ES-T (accelerometer)	Kinemetrics EpiSensor ES-T (accelerometer)	00(Surface): Kinemetrics EpiSensor ES-T; 01(–42 m): Kinemetrics EpiSensor ES-SB; 02(–550 m): Kinemetrics EpiSensor ES-DH; (accelerometers)	Strekeisen STS-2–120S (seismometer)	MoHo Tromino 3G (seismometer)
Digitizer	Nanometrics Centaur	Nanometrics Taurus	00, 01, 02: Nanometrics Centaur	Kinemetrics Quanterra Q330	–
Frequency range (according to manufacturer)	[DC, 250] Hz	[DC, 250] Hz	[DC, 250] Hz	[0.00833, 50] Hz	[0.03, 50] Hz
Sensor housing	Big pot, concrete vault	Building (concrete slab)	00: concrete slab 01, 02: borehole	Building	Free-field

in Table 1. When several seismic stations are present on a same basin, we selected the station closer to the valley centre, where the amplitude of the odd vibration modes is generally larger (Fig. 1).

Since seismic sensors at permanent stations are usually oriented towards north, the recorded time-series were rotated along the basin principal axes (longitudinal and transverse, Fig. 1) before being used.

We also note from Fig. 2 that some stations contain accelerometric sensors (SEFS, SIOO and OGFO) and other stations contain seismometers. Accelerometers are known to have larger intrinsic noise (Ringler *et al*. 2015) and they are intended for strong motion recordings. This should be recalled when analysing accelerometric data. However, in this study, as we will show, we did not experience limitations due to the larger intrinsic noise of accelerometers.

Some stations are set in free field (SEFS and GARG), others on the foundations of multistorey buildings (SIOO and BOSI). The OGFO station in the Grenoble basin is equipped with three sensors, one on the surface (OGFO-00), currently working and two in borehole, at 42 m (OGFO-01) and 550 m depth, on the bedrock (OGFO-02). The latter two ceased functioning in February 2017.

From now on, for the sake of simplicity we refer to the basins with their seismic station acronym (SEFS, SIOO, OGFO, BOSI and GARG).

2.1 Modal frequency identification in the amplitude spectra

In Fig. 3, we show the typical velocity amplitude spectra recorded at the selected stations. The local resonances appear as distinct peaks in the main (longitudinal, transversal and vertical) directions. Their uncertainty will be discussed in the following section. As already pointed out, we did not perform any new modal recognition, but relied on more comprehensive studies performed by the authors listed in Fig. 2.

At SEFS, the L1, T1, V1 frequencies can be recognized (Fig. 3). L1 an T1 perfectly match those already described in the seismic station report (Hobiger & Fäh 2020). The spectra computed on 1, 6 and 12 hr time intervals of random days in the 5 analysed years all exhibit the same main peaks.

At SIOO, the L1, T1, V1 frequencies can be easily recognized, while at OGFO only the fundamental modes L1 and T1 can be recognized. We note that this is the basin with the lowest aspect ratio among those investigated.

BOSI and GARG are two stations located along the river Adige valley in Italy. They are only 20 km apart but show two different modal frequency patterns, indicating different underground geometries at the two sites. At BOSI, only L1 and T1 frequencies can be identified, while at GARG also the L2, L3 frequencies can be seen.

3 RESULTS

3.1 Time stability of stratigraphic modal frequencies

In order to find the most suitable processing parameters, we computed the spectra by using 30 min, 1 hr, 6 hr, 12 hr and 24 hr time-segments. The window length was adapted to retain a fixed number of windows in the analysis for each case. We found that the uncertainty in the modal frequency assessment decreased from a few per cent to a few per thousand as per Table 2. We thus decided to work with 6 hr segments.

Then, we computed the spectra in the UTC 00:00–6:00 a.m. interval (to reduce anthropic noise) for 5 yr (2017–2022) at all the inspected sites, with the only exception of GARG, where only 18 months of data were available (Fig. 4). Each 6 hr data segment was split into 36 ten-minute windows, detrended, tapered, FFT-transformed and smoothed (according to a rectangular window with a width equal to 3% of the central frequency). The final spectrum for each day is the average of the 36 windows. In this way the spectral resolution is 0.0017 Hz.

An automatic picking of the maximum spectral valueswas carried out in predefined frequency intervals, wide enough to identify the eigenfrequencies of interest.

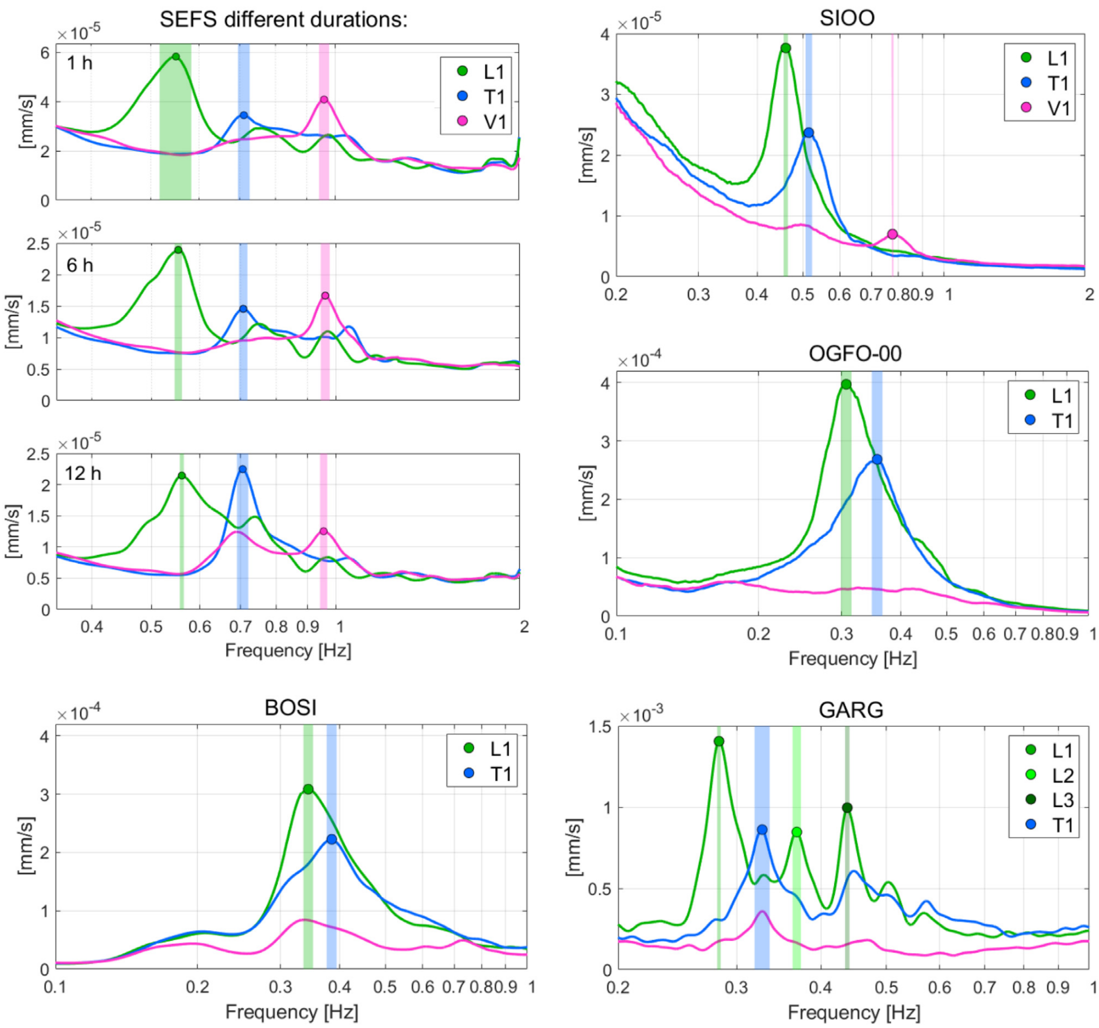

Figure 3. Average spectral components of motion (green: longitudinal, blue: transversal, magenta: vertical). The main identified eigenfrequencies for each site are marked by the dots. The coloured vertical bands indicate the standard deviation of the peak frequencies computed on 36 ten-minute long windows, in a 6-hr random day recording. The top left panels, referring to the SEFS site, show how this standard deviation becomes smaller, particularly for low frequency modes, by increasing the time considered for the computation.

Table 2. Uncertainties in the modal frequency assessment by the peak-picking procedure on the amplitude spectra when these are obtained from 30 min, 1 hr, 6 hr, 12 hr, 24 hr segments. The values are indicative for the fundamental modes L1, T1.

30 min	1 hr	6 hr	12 hr	24 hr
5 %	3.5 %	0.6 %	0.6%	0.5%

Values beyond 3σ have been considered as outliers and discarded from the following calculations. These correspond to instrumental malfunctioning or nuisance close to the seismic stations.

In total, less than 50 d in 5 yr were discarded, except for OGFO where the data were more disturbed, and 200 d had to be removed.

Resonances are intrinsic properties of sedimentary bodies and hence they should be stable over time, as long as the sedimentary bodies do not change. Less obvious is that they are still stable under non-stationary forcing conditions, such as those imposed by microtremor. Fig. 4 shows that the eigenfrequencies identified in the studied basins are very stable: they can be recognized, *de facto*, any day. They can clearly be identified both at the scale of few hours (or fraction of hours, Table 2) and at multiyear timescale (Fig. 4, Table 3).

However, another interesting feature emerges by closely examining the spectrograms: eigenfrequencies show a remarkable annual fluctuation, increasing in summer and decreasing in winter.

This pattern is even clearer for higher modes; this could also, at least in part, be due to the fact that these are more sensitive to the shallow stratigraphy, that high frequencies have a better spectral resolution and that instrumental sensitivity (particularly for accelerometers) is larger at higher frequencies.

The seasonal variation in the eigenfrequencies is less evident (around 1 per cent) on the low aspect ratio basin (OGFO) and at BOSI, which lies at the intersection of 2 valleys (Fig. 2). The seasonal variation shows the largest relative amplitude at SEFS, where it reaches about 5 per cent in frequency.

The frequency fluctuation is also appreciable on a daily scale, although less pronounced (e.g. around 3 per cent at SEFS) with a relative increase of the modal frequencies in the daytime hours compared to night-time (Fig. 5). The maximum frequency value is reached at about 2 pm local time, the minimum at about 2 am local time.

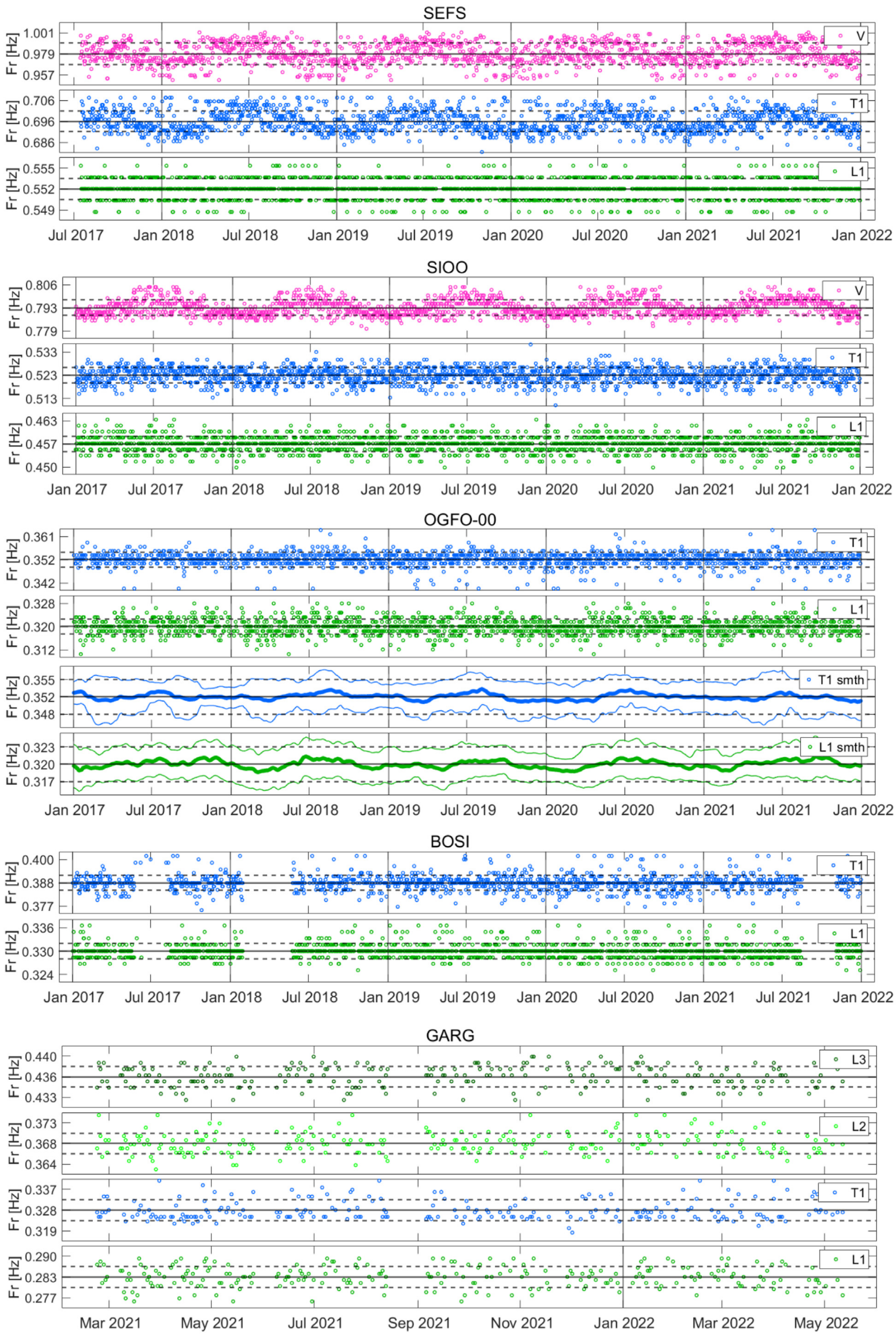

Figure 4. Main modal frequencies identified at the inspected sites over 5 yr. Longitudinal modes are in shades of green, transversal modes in blue and vertical modes in magenta. The mean values throughout the 5-yr analysis are given by the black thick horizontal lines, the standard deviation by the horizontal dashed lines. OGFO eigenfrequencies have been smoothed with a 60-d moving window to better visualize seasonal trends.

Table 3. Standard deviations of the main modal frequencies at the selected basins computed in the whole 5-yr interval considered.

	SEFS	SIOO	OGFO	BOSI	GARG
Frequency variation (%)	V1: 1.11% T1: 0.71 % L1: 0.27 %	V1: 0.81% T1: 0.95 % L1: 0.65 %	T1: 1.26 % L1: 1.23 %	T1: 1.52 % L1: 0.90 %	L3: 0.45 % L2: 0.81 % T1: 1.50 % L1: 1.05 %

The cross-correlation between the temperature and the L1, T1, V1 modal frequencies for the whole month of July 2020 is shown in Fig. 6 (top panel) for the SEFS station. We chose July because it is the month in which the daily variation in temperature is the largest. The spectra of the cross-correlation series exhibit a 24-hr periodicity, as temperature (Fig. 6, top panel) and the typical time-lag between the two series is about 5 hr or 24–5 = 19 hr, depending on the point of view. In a recent work also Xiao & Wang (2022) documented HVSR daily fluctuations on Mars, where the daily temperature varies between −83 and 13°C.

3.2 Time stability of non-stratigraphic modal frequencies

It is curious but also very important to note that the recordings of the seismic stations do not show only stratigraphic features. When hosted inside structures, they typically contain also the natural vibration modes of the surrounding structures (Castellaro *et al.* 2022). This is the case of BOSI and SIOO, where the 2.9 and 3.9 Hz peaks that can be observed in the horizontal spectral components are the natural modes of the hosting buildings (Fig. 7). This is known, for the BOSI site, from previous surveys. For SIOO this has been inferred from the building geometry and other considerations on the spectral features that differ considerably between stratigraphic and non-stratigraphic peaks (Castellaro & Mulargia 2010; Castellaro 2016a; Castellaro *et al*. 2022). These frequencies, too, show a marked annual fluctuation. Differently from the stratigraphic modal frequencies, annual variations of structural modal frequencies are well-known features, discussed by many authors (e.g. Ramìrez *et al*. 2022, for a recent review). In the case of structures, the seasonal variation is undoubtedly, at least in part, related to temperature, since the elastic moduli of many structural materials change significantly with temperature. The annual fluctuations of the resonance frequencies due to the surrounding structures at SIOO (5.2 per cent) and BOSI (4.5 per cent) are larger than those of stratigraphic origin, though with the same trend, increasing in summer and decreasing in winter.

What is opposite, compared to the stratigraphic cases is the spectral amplitude. While for the stratigraphic peaks we observe an amplitude increase in winter, due to a higher atmospheric excitation level (the Appendix), at SIOO the building modal amplitude is larger in summer. This can possibly be due to the extra-excitation coming from the air conditioning systems of the ophthalmology hospital hosting the seismic station.

This example is discussed here to stress out that distinguishing stratigraphic from non-stratigraphic spectral peaks is a mandatory step before any data interpretation, also at seismic stations.

4 DISCUSSION

The modal frequencies recognizable at the inspected basins can be detected any day of the year and can be assessed with a precision Δf ranging from 1 to 5 per cent, depending on the duration of the acquisition. However, such variation is not only due to experimental uncertainties but is also linked to an apparently real variation of the modal frequencies that increases in summer and decreases in winter at all the sites belonging to the alpine and subalpine investigated regions. Such variation explains from 0.3 to 1.5 per cent of the total observed variation Δf and is larger for higher modes, compared to fundamental modes. Such variation can also be observed at the daily scale, where it explains approximately 1 per cent of the total observed variation Δf.

It is well known that the natural vibration frequencies and mode shapes of linear elastic bodies can be derived as stationary harmonic solutions of the following system of linear differential equations $[m]\ddot{x} + [c]x + [k]x = 0$, where $[m]$, $[k]$ and $[c]$ are the mass, the stiffness and the damping matrices and x is the generalized coordinate vector. From these, it comes that the natural frequencies of a simple harmonic oscillator are:

$$\omega_0 = \sqrt{\frac{k}{m} - \frac{c^2}{4m^2}}. \quad (1)$$

This means that the frequency increase that we observe in summer could be explained by: (1) a stiffness increase of the resonating sedimentary fill or (2) a mass decrease or (3) a damping decrease or (4) an increased tension applied to the sediment-filled basin (this is not indicated by the equation above but still well known in the elastic theory).

We identified several possible hypotheses, both of external origin (atmospheric load, temperature and water level) and instrumental issues (instrumental clock drifts, thermal drift of other electronic components), to explain the observables, which we discuss below. We observe that plausible hypotheses should ideally explain both the seasonal and the diurnal observed oscillations, though there can be factors affecting more the former than the latter, and vice versa.

1) Variation of the atmospheric load on the valleys between summer and winter. The seasonal barometric fluctuation in the studied areas is, on average, less than 5 kPa. This is equivalent to an increase/decrease in mass lower than 1 m of soil. The annual 'static' load variation can hardly be responsible for the seasonal modal frequency variations observed and cannot explain the daily variation that was found.

2) Direct thermal effects on the basin and/or surrounding rocks. It has been suggested that finite thermo-elastic (Berger 1975; Ben-Zion & Leary 1986; Richter *et al.* 2014) and poro-elastic (Roeloffs 1988) strain causes changes in the shear modulus of geological materials. Berger (1975) suggested that, although annual temperature variations do not penetrate far into the soil, the indirect effect of thermal stress may affect much deeper strata. In the presented cases 'deeper' should however mean several hundred meters.

A direct effect of air temperature on the vibration frequencies of rock columns was documented by Bottelin *et al.* (2013) and Colombero *et al.* (2018). The former described seasonal fluctuations of a 6 Hz resonance, with a 3-month lag compared to the air temperature maxima. They attributed this behaviour to the variation of the rock elastic moduli with temperature, which is anticorrelated with temperature, thus giving larger frequencies in winter. The latter observed daily and seasonal fluctuations of the 4 Hz eigenfrequency of a rock cliff and attributed it to the thermally induced opening and closing of rock mass fractures.

Vassallo *et al.* (2022a, b) also described seasonal frequency fluctuations on high-frequency microtremor H/V peaks recorded at two

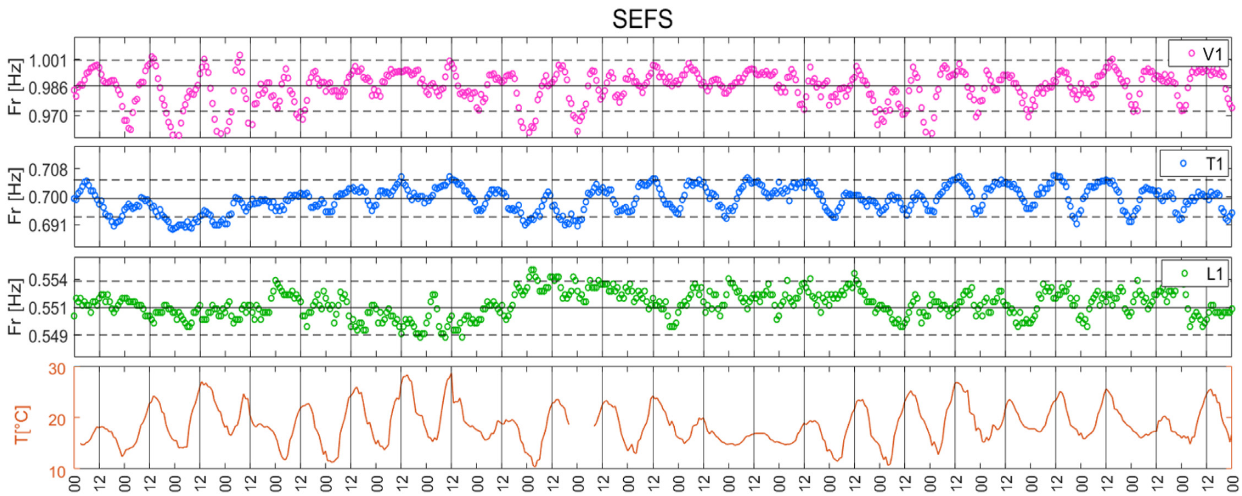

Figure 5. Main modal frequencies L1, T1, V1 identified at SEFS in July 2020. Each dot corresponds to an eigenfrequency value measured in 1-hr segment. The mean values over the 1 month analysis are given by the black horizontal line, the standard deviation by the horizontal dashed lines. The bottom panel shows air temperature measured at Altdorf (WMO 0 6672), 5 km from SEFS; for the same time interval.

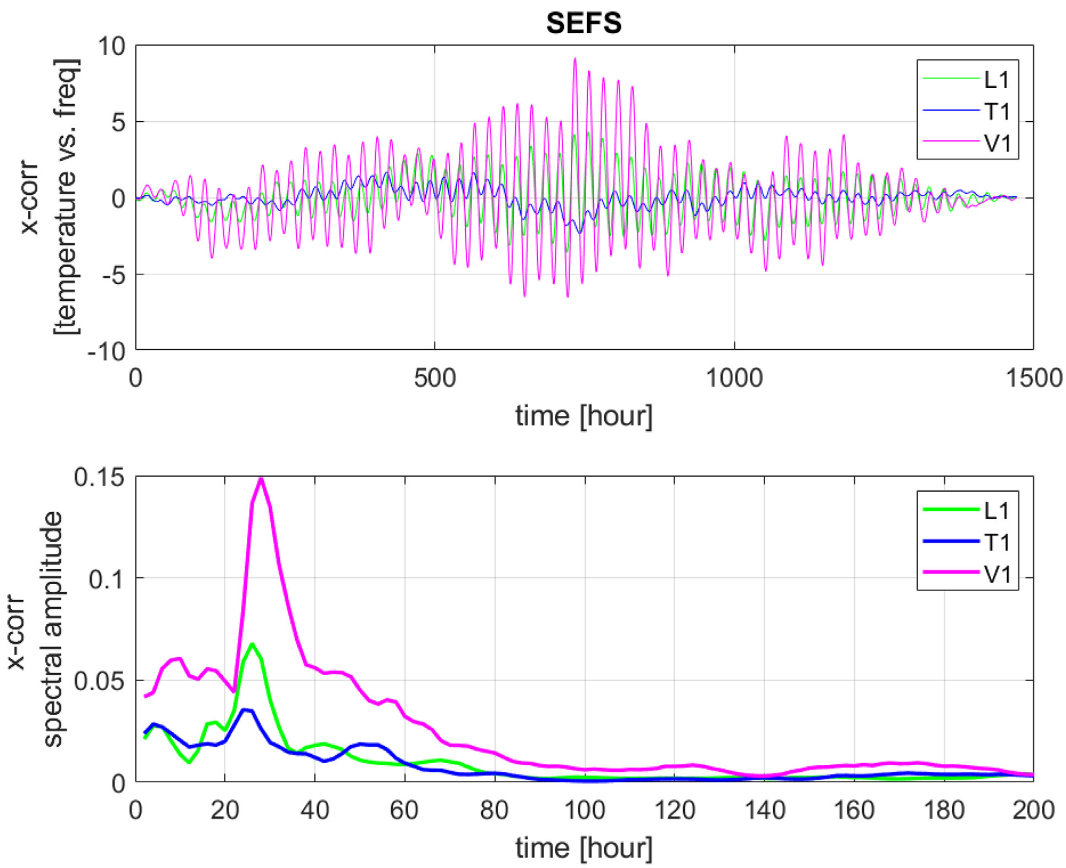

Figure 6. Top panel: cross correlation between temperature and L1, T1, V1 frequencies for the month of July 2020. Bottom panel: spectra of the cross-correlation functions showing a remarkable periodicity of 24 hr (1 d).

seismic stations and described a 20–40 d (Vassallo *et al.* 2022a) and a 70–90 d (Vassallo *et al.* 2022b) phase lag between the frequency and the temperature peaks.

However, while a thermal origin for these observations appears credible, this is less plausible in alpine basins hundreds of meters thick, where the annual change in temperature cannot be significant below 10 m depth (Hillel 2013). In addition, these hypotheses applied to our case would imply that the basins respond to thermal fluctuations with a delay of 6 months in the case of the seasonal variations.

3) Indirect thermal effects on the basin (phreatic and artesian aquifer). In plain areas, in the Northern Hemisphere, a reduction of the water content, and a lowering of the water table, is expected in

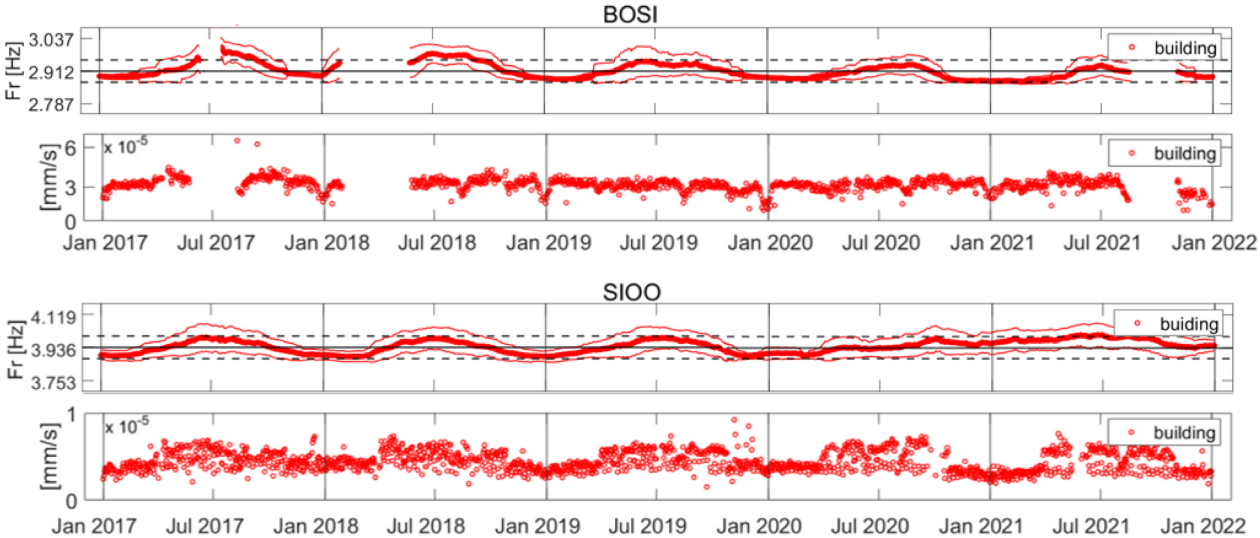

Figure 7. Horizontal non-stratigraphic (i.e. building) spectral frequency and amplitude peak variation at BOSI and SIOO. The frequency time-series is provided in terms of mean ±1 standard deviation while the amplitude time-series is provide as computed, hour after hour and day after day. From the amplitude behaviour, it is clear that the BOSI building is almost empty during the Christmas and New Year eve days and around August 15th, which is national holiday in Italy.

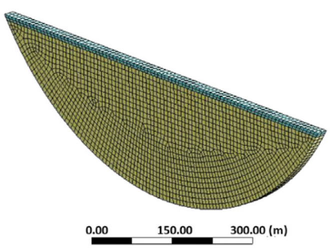

MODEL A - PARAMETERS				
Circular; w = 450 m; h = 225 m; h/w = 0.5				
Layer		ρ $[kg/m^3]$	V_S $[m/s]$	ν
1	10 m, wet	2100	300	0.477
1	10 m, dry	2000	300	0.451
2	wet	2000	500	0.440

MODEL A - RESULTS				
	L_1 $[Hz]$	L_2 $[Hz]$	L_3 $[Hz]$	T_1 $[Hz]$
All wet	0.635	0.882	1.131	0.794
Layer 1 dry, layer 2 wet	0.637	0.884	1.135	0.796
Δf [%]	**0.22%**	**0.26%**	**0.30%**	**0.20%**

MODEL B - PARAMETERS				
Circular; w = 1250 m; h = 500 m; h/w = 0.4				
Layer		ρ $[kg/m^3]$	V_S $[m/s]$	ν
1	10 m, wet	2100	300	0.477
1	10 m, dry	2000	300	0.451
2	wet	2000	700	0.400

MODEL B - RESULTS				
	L_1 $[Hz]$	L_2 $[Hz]$	L_3 $[Hz]$	T_1 $[Hz]$
All wet	0.416	0.539	0.664	0.485
Layer 1 dry, layer 2 wet	0.417	0.540	0.666	0.486
Δf [%]	**0.22%**	**0.25%**	**0.28%**	**0.21%**

Figure 8. Mechanical parameters and results for two finite element models of circular cross-shape water saturated sedimentary basins simulating a 10 and 20 m water table drop. Model A reproduces the SEFS case study. w is the basin half-width, $\boldsymbol{h}$ the basin maximum thickness, $\boldsymbol{h/w}$ the aspect ratio, $\boldsymbol{\nu}$ the Poisson's ratio, $\boldsymbol{L_i}$, $\boldsymbol{T_i}$ the frequency of the longitudinal and transversal modes.

summer. This reduces the mass and would translate into a resonance frequency increase.

However, as a consequence of the snow melt, the water table rises in summer compared to winter at all the inspected sites, as documented by the annals of the local hydrological observatories.

At SEFS the water table has an average annual fluctuation lower than 2 m, with summer maxima (MONITRON 2018). At SIOO the annual fluctuation is less than 3 m, again with summer maxima (Fette 2005) and at BOSI less than 5 m, always with summer maxima (Comune di Bolzano 2018).

We run two finite element models of circular basins with aspect ratio 0.5 and 0.4 (model A and model B in Fig. 8, with the same principles described in Castellaro & Musinu 2022), to replicate the cases of SEFS and SIOO, respectively, where the observed frequency fluctuations are the largest. We set the densities, shear wave velocity and elastic moduli to values collected from the literature, where available, and capable to replicate the experimental modal frequencies. We first run the models in the case of totally saturated soil. Then, we set the upper 10 and the upper 20 m to a dry condition, as to mimic a water table drop of 10 and 20 m, respectively. We see that the maximum natural frequency variation explained by such a large water table variation is 0.3 per cent, which is significantly lower that what we found experimentally, even if the water table drop applied to the model is at least two to four times larger than what measured in the real cases. Additionally, which is more important, the rise of the water table implies a decrease of the resonance frequencies, which is theoretically obvious, but which is opposite to the experimental evidence, where frequencies increase when also the water table rises.

In addition, in no way could the water table movement explain the observed diurnal modal frequency variations (Fig. 5).

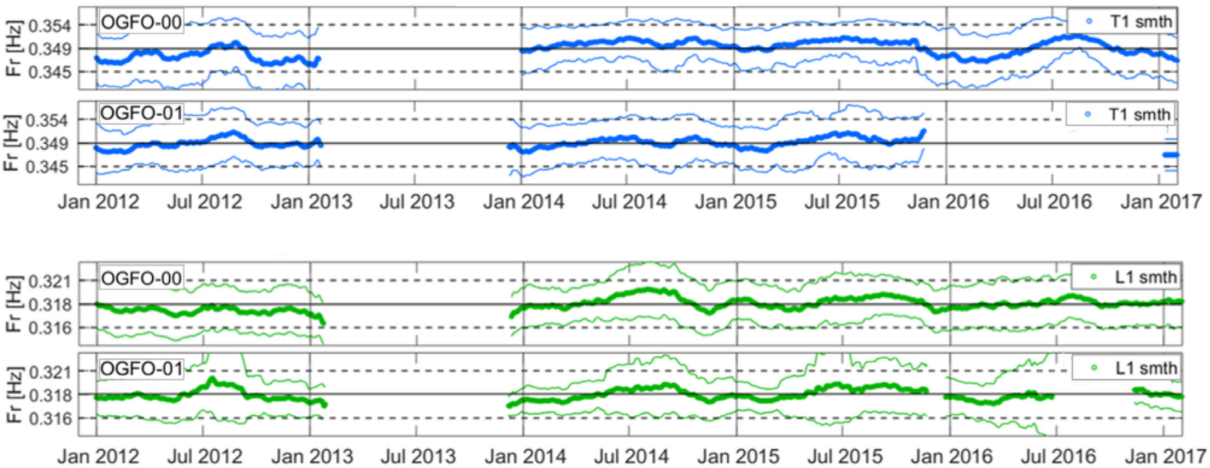

Figure 9. Temporal stability of eigenfrequencies at OGFO-00 (surface) and at OGFO-01 (−42 m depth) in the time interval when both stations worked simultaneously. Longitudinal modes are in green and transversal modes in blue. Eigenfrequencies mean and standard deviation are shown by the horizontal solid and dashed black lines. Data were smoothed with a 60-d moving window in order to better visualize seasonal trends (60-d moving average and standard deviation in colour).

As known, the effective tension applied on a soil under water is the difference between the total load and the neutral pressure $\sigma_{\text{eff}} = \sigma_{\text{tot}} - u$ (Terzaghi 1923). This means that when the water table rises (summertime), the effective stress decreases. A decrease in the tension applied to the soil deposits also imply a decrease in the corresponding eigenfrequencies. This is a second order effect and, according to our calculations, it would explain less than 0.1 per cent of the observed phenomenon but again with an 'opposite sign'.

Thus, according to our calculation, the water table changes cannot explain neither the diurnal nor the seasonal observational evidence. In the last case, they even have an opposite trend.

4) Indirect thermal effects on the basin (soil drying, overconsolidation). Fine grained sediments (clays) are known to become very stiff when dried. When outcropping, this usually leads to very stiff soils in the upper 1-2 m in summer compared to winter. All the inspected basins, being in the mountains, are mostly filled with sandy-gravelly sediments in the upper parts. However, by using the same modelling principles described for item 3), we modelled a cap of 5 m thickness clay with winter-to-summer Vs increasing from 150 to 180 m/s. This would lead to an increase of L1 frequency of 0.06 per cent and of T1 frequency of 0.08 per cent. A Vs increase from 150 to 300 m/s would imply a frequency increase of 0.39 and 0.55 per cent for L1 and T1, respectively (see also Saul & Lumley 2013; Bertello *et al*. 2019).

Thus, in principle clayey caps drying in summer could be responsible for some modal frequency increase. However, 5 m is certainly a thickness overestimation, as well as Vs doubling their values in summer compared to winter. Also, the lateral continuity of any plausible clayey cap in so big basins would be largely questionable. In addition, this phenomenon could not explain the observed diurnal frequency fluctuation.

5) Forcing effect. Damping (c in eq. 1) is known to vary both with the frequency and amplitude of motion. The larger they are, the larger the damping. Larger damping implies a decrease in resonance frequencies (eq. 1). Then, one can expect that in summertime, when the amplitude of motion is generally lower on the basin due to less atmospheric perturbations (see the Appendix), damping is lower, and frequencies become higher. In principle this phenomenon would support the experimental fluctuation observed in the basins. However, as we show in the Appendix, damping measured as proposed by Chopra (1995) increases in summertime. This indicates that, in the analysed basins and under microtremor conditions, the damping is not primarily controlled by the amplitude of motion and also this possible explanation fades.

Since no apparently convincing external-only explanations can be found, we move to other possible internal (to the instrumental chain) explanations.

6) Thermal drift of the digitizer clock, controlling sampling rate. Digitizer clocks are traditionally based on quartz or similar oscillators and are known to suffer from thermal drift. However, this effect should be well compensated in modern seismological digitizers that are connected and corrected in real time on GPS clock basis (Ringler *et al.* 2021).

7) Thermal effect on the force-balance circuit electronic components. The digitizer clock is not the only thermal-sensitive component in a seismic instrumental chain. Any other electronic component (capacitors, resistances, time-constants etc.) is affected by temperature variations. The most notable thermal effect on digitized signals is the offset (baseline) variation that is easy to compensate. As far as we could see, no studies on possible frequency drifts other than those listed on item 6) above appear in the literature or in the instruments user's manuals.

We also analysed the data of the station OGFO-01, where the sensor is placed at 42 m depth. In Fig. 9 these are compared with OGFO-00, which is the station on surface, for the time in which the recordings were simultaneous. If the modal frequency variation were an air temperature-controlled effect, we would expect to see no seasonal variations in the data from the sensor placed at 42 m depth (OGFO-01) but this is not the case. The underground station still shows annual oscillations in the recorded basin eigenfrequencies. However, it has to be noted that only the sensor is placed inside the hole, at 42 m depth. The digitizer and the rest of the instrumental

Table 4. Average modal frequency variations and outdoor air temperature at the selected stations.

	SEFS	SIOO	OGFO-00	OGFO-01	BOSI
Sensor position	'Open air' (concrete vault)	Indoor+ thermostatic box	'Open air'	Sensor in hole - Digitizer on surface	Indoor+thermostatic box
Aspect ratio	0.50	0.37	0.22	0.22	0.40
Average modal frequency variation	$\Delta f_{V1} = 4.7\%$ $\Delta f_{T1} = 3.1\%$	$\Delta f_{V1} = 1.8\%$ $\Delta f_{T1} = 2.1\%$	$\Delta f_{T1} = 0.9\%$ $\Delta f_{L1} = 0.6\%$	$\Delta f_{T1} = 1.1\%$ $\Delta f_{L1} = 0.9\%$	No fluctuations
Average air ΔT (summer–winter)	28 °C	30 °C	28 °C	28 °C	28 °C
Meteo station	Altdorf (WMO 06672)	Sion (WMO 06720)	Grenoble (WMO 07487)	Grenoble (WMO 07487)	Bolzano (WMO 16020)

chain are all set on surface; therefore we cannot exclude an air temperature-control on these parts.

Among the analysed seismic stations, BOSI and SIOO are placed in thermostatic boxes on the building basements, while SEFS and OGFO-00 are just protected by their shelters, with no insulation boxes. The average temperature difference between summer and winter, ΔT, at all the selected stations is around 28 °C. By looking at Table 4 we observe that, in general, the larger the aspect ratio of the basin, the larger its modal frequency variation and that ΔT alone is apparently not the only parameter governing the size of the seasonal frequency variation.

At present we are planning to conduct an experiment in thermally controlled rooms to test the effect of temperature variations (beyond the already known baseline shift) on the instrumental chains (sensors and digitizers) in long-term acquisitions.

5 CONCLUSIONS

We analysed multiyear time-series of seismic stations installed on alpine basins with aspect ratios ranging from 0.2 to 0.5, to study the recognizability of the basin natural frequencies and their stability over time. Natural frequencies are intrinsic properties that need to be excited to be measured (in this way they become resonances). The question was whether ambient noise, which is not a white function, excites those frequencies enough to make them visible any day of the year.

We found that the natural vibration frequencies in the investigated alpine basins (all <1 Hz) are visible throughout the considered time, both using long (hours) and short (30 min) time-series, with uncertainties ranging from 1 to 5 per cent in the two cases. In this type of basins, the spectral shape of the exciting function (microtremor), which is not white, does not affect the visibility of the natural vibration modes.

This is an important result because it empirically shows that the observable natural modes are, in practice, independent from the forcing functions when this is microtremor (while their amplitude and damping depend on them, see Appendix), at least for this type of inspected basins.

We note that we refer only to natural frequencies larger than 0.2 Hz, since below this frequency the oceanic peaks (Longuet-Higgins 1950; Haubrich *et al.* 1963) may dominate the scene.

A very interesting fact emerged from the analysis: modal frequencies show an evident seasonal trend, particularly, but not exclusively, affecting the transversal and vertical directions. The frequencies become larger in summer compared to winter, in the alpine and subalpine investigated regions. Higher modal frequencies seem to be more affected by this fluctuation, but this could also be due to a better spectral resolution at higher frequencies. The frequency fluctuation is also appreciable on a daily scale, although less pronounced, with a relative increase of the modal frequencies in the daytime hours compared to night-time.

Annual trends in modal frequencies or in H/V ratios have already been documented by some authors (Bottelin *et al.* 2013; Colombero *et al.* 2018; Vassallo *et al.* 2022a,b) but restricted to frequencies more than one order of magnitude larger than those described here. Due to the very different wavelengths involved, the causes behind the two phenomena could even be different. Apparently, a daily fluctuation has instead never been documented before.

We observe that what we identified as 'resonances', in the large aspect-ratio sediment-filled basins analysed, are typically real (*P*, *S* waves) resonance and not surface-wave trapping phenomena (Bard & Bouchon 1985; Sgattoni e Castellaro 2020). The former are characterized by peaks in the individual spectral components of motion, while surface-wave trapping phenomena are typically marked by H/V peaks, due to local minima in the vertical spectral component (Castellaro 2016b). The type of seismic waves and their penetration depth is different in the two cases. In the second case the reasons for the observed frequency variations could be looked for near surface, compared to the first case (which is the case that we are discussing here).

We evaluated a series of possible explanations for this phenomenon, both of external origin (atmospheric load, temperature, water level and soil moisture) and instrumental issues (instrumental clock drifts, thermal drift of other electronic components). We showed, for example, that the seasonal variation of the water level would produce a modal frequency variation opposite to what we found and, in any case, capable to explain only a fraction of the observed variation.

If the air temperature variation affects the electronic components behaviour of seismometers, we would not expect to see any variation at in-hole stations while we still see it. This wouldin principle suggest that the thermal effect is not affecting the sensors but the digitizers, which are located on the surface.

At the time of writing, we cannot suggest a clearly dominant hypothesis over the others, and the experimental evidence likely reflects the combined effect of more than a single hypothesis. However, a number of reasons that could explain the annual trend have to be discarded when applied to the daily trend. As this paper article goes to press, Kramer *et al.* (2023) propose that the combined effect of air pressure and ground water can explain the shear wave velocity in the subsoil at the sub-daily scale. This stiffness variation of subsoil can certainly affect the resonance frequencies. However, the phenomenon they describe affects frequencies much larger than those presented in the present study.

The hypothesis that the observed frequency wandering could in part have an instrumental origin cannot be fully discarded at

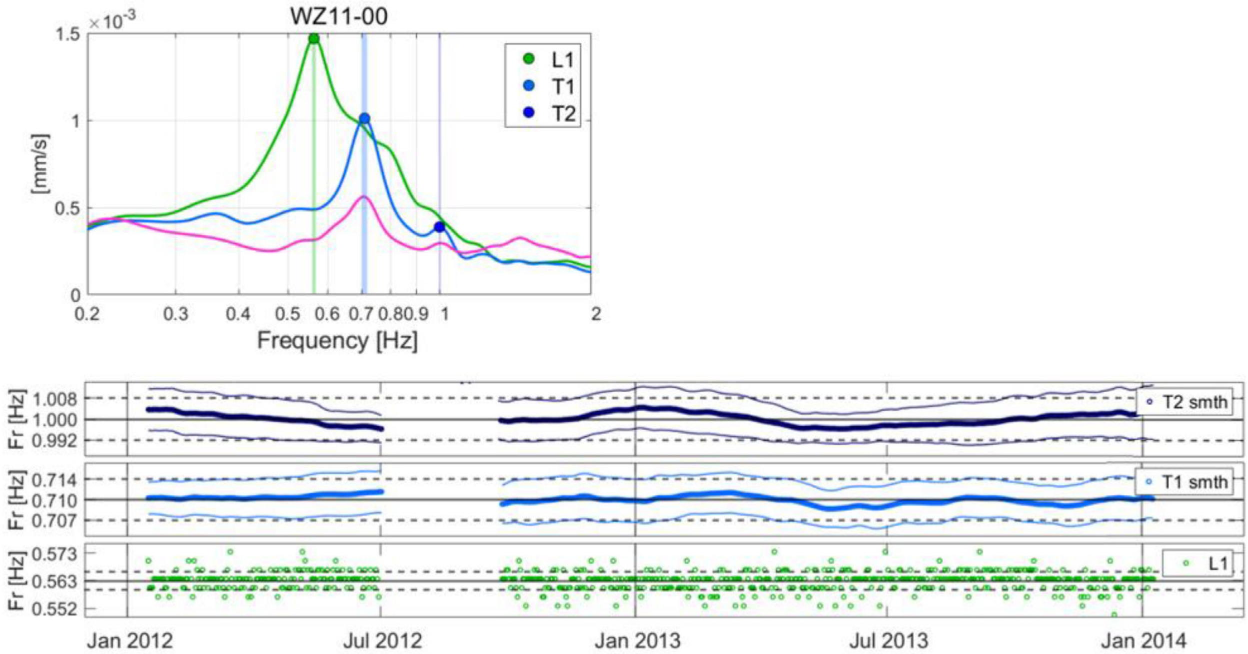

Figure 10. Top panel: average spectral components of motion (green: longitudinal, blue: transversal, magenta: vertical) at WZ11-00 (New Zealand). The main identified eigenfrequencies are marked by the dots. The coloured vertical bands indicate the standard deviations computed on 36 ten-minute long windows, in a 6 hr random day recording. Bottom panel: main modal frequencies identified at WZ11-00 on the time interval analysed. Longitudinal modes are given in green, transversal modes in blue and vertical modes in magenta. The mean values throughout the 5-yr analysis is given by the black thick horizontal line; the standard deviation by the horizontal dashed lines. T1 and T2 have been smoothed with a 60-d moving window to better visualize seasonal trends.

this stage. BOSI station supports this statement: at BOSI we did not observe any annual or diurnal frequency wandering. BOSI is the only station located on the basement of a structure (where the thermal excursion affecting the instrument is thus expected to be low) and protected by a styrofoam box, according to the STS-2 installation recommendations.

All the other instruments are not specifically protected against temperature variations.Thermally isolating seismic sensors was and still is normal for long period sensors (like STS-2) but is no more applied to short period seismometers and accelerometers. Operators usually pay attention to apply baseline corrections to compensate for the offset variation due to thermal drifts but we have not found any study on the frequency response stability of these instruments with temperature.

The research is still open. We plan to study other valleys and the thermal response of the instrumental chains in the attempt to come to an answer.

In the meanwhile, to check whether this phenomenon could be observed also in the opposite hemisphere and with an opposite trend (being the temperature pattern reversed there), we searched for similar sediment-filled basins equipped with seismic stations therein. In Fig. 10 we show the natural frequency stability of the Whataroa basin in New Zealand, as measured by the local seismic station WZ11-00. Here, modes T1 and T2 shift towards larger frequencies in January–February, that is opposite to what happens in the northern hemisphere, as expected for thermally controlled phenomena.

We conclude by stating that in 2-D sedimentary basins like those investigated, the modal frequencies can be inferred with confidence even in extremely short (30 min) measurements, with a few per cent uncertainty and that part of this uncertainty is due to a real frequency wandering over time (typically correlated to air temperature) of still unclear origin.

DATA AND RESOURCES

The seismic station data were downloaded from the online platform IRIS.edu (last accessed: 11 March 2023), with the exclusion of the GARG data that were personally collected by the authors with the help of Bogomil Brecelj. Temperature data were downloaded from Meteostat.net weather and climate database. The data can be made available upon request to the authors.

ACKNOWLEDGMENTS

We sincerely thank Laura Ermert and the anonymous reviewer for their recommendations, which helped us improving the paper. We sincerely thank Bogomil Brecelj for hosting and taking care of the seismic station at GARG. We thank Giuseppe Musinu for his help with the computations behind Fig. 8. We thank Professor Emelin Maufroy for detailed information about OGFO stations. We thank Sandro Rao (INGV) and Lunger Walther (provincia di Bolzano) for providing us materials about BOSI and John Francis Clinton (SED-ETH) about SEFS and SIOO.

REFERENCES

Bard, P.Y. & Bouchon, M., 1985. Bull. Seismol. Soc. Am.The two-dimensional resonance of sediment-field valleys, *Geophys. J. Int.,* **75,** 519–541.

Ben-Zion, Y. & Leary, P., 1986. Thermoelastic strain in a half-space covered by unconsolidated material, *Bull. seism. Soc. Am.,* **76**(5), 1447–1460.

Berger, J., 1975. A note on thermoelastic strains and tilts, *J. geophys. Res.,* **80**(2), 274–277.

Bertello, L., Berti, M., Castellaro, S. & Squarzoni, G., 2019. Dynamics of an active earthflow inferred from surface wave monitoring, *J. geophys. Res.,* **123,** 1811–1834.

Bottelin, P., Levy, C., Baillet, L., Jongmans, D. & Gúeguen, P., 2013. Modal and thermal analysis of Les Arches unstable rock column (Vercors massif, French Alps), *Geophys. J. Int.,* **194**(2), 849–858.
Castellaro, S., 2016a. Soil and structure damping from single station measurements. *Soil Dyn. Earthq. Eng.,* **90,** 480–493.
Castellaro, S., 2016b. The complementarity of H/V and dispersion curves, *Geophysics,* **81,** T323–T338.
Castellaro, S., Alessandrini, G. & Musinu, G., 2022. Seismic station installations and their impact on the recorded signals and derived quantities, *Seismol. Res. Lett.,* **93,** 3348–3362,
Castellaro, S. & Mulargia, F., 2010. How far from a building starts the tremor free-field? The case of three most famous Italian towers and of a modern building, *Bull. seism. Soc. Am.,* **100,** 2080–2094.
Castellaro, S. & Musinu, G., 2023. Resonance vs. shape of sedimentary basins, *Bull. Soc. seism. Am.,* **113**(2), 745–761.
Chopra, A.K., 1995. *Dynamics of Structures: Theory and Applications to Earthquake Engineering,* Prentice-Hall.
Colombero, C., Comina, C., Vinciguerra, S. & Benson, P.M., 2018. Microseismicity of an unstable rock mass: from field monitoring to laboratory testing, *J. geophys. Res.,* **123**(2), 1673–1693.
Comune di Bolzano, 2018. Stato della falda acquifera di Bolzano, Available at: http://www.comune.bolzano.it/print_context.jsp?ID_LINK=4172&area=69&page=1&id_context=22673, last accessed, July 2022.
Delépine, N. & Semblat, J.F., 2012. Site effects in an Alpine valley with strong velocity gradient: interest and limitations of the 'classical' BEM, *Soil Dyn. Earthq. Eng.,* **38,** 15–24.
Di Giulio, G., de Nardis, R., Boncio, P., Milana, G., Rosatelli, G., Stoppa, F. & Lavecchia, G., 2016. Seismic response of a deep continental basin including velocity inversion: the Sulmona intramontane basin (Central Apennines, Italy), *Geophys. J. Int.,* **204**(1), 418–439.
Ermert, L., Poggi, V., Burjánek, J. & Fäh, D., 2014. Fundamental and higher two-dimensional resonance modes of an Alpine valley, *Geophys. J. Int,* **198,** 795–811.
Fette, M.W., 2005. Tracer Studies of River-groundwater Interaction under Hydropeaking Conditions, *Doctoral dissertation,* ETH Zurich.
Gúeguen, P., Cornou, C., Garambois, S. & Banton, J., 2007. On the limitation of the H/V spectral ratio using seismic noise as an exploration tool: application to the Grenoble valley (France), a small apex ratio basin, *Pure appl. Geophys.,* **164,** 115–134.
Haubrich, R.A., Munk, W.H. & Snodgrass, F.E., 1963. Comparative spectra of microseisms and swell, *Bull. seism. Soc. Am.,* **53**(1), 27–37.
Hillel, D., 2013. *Introduction to Soil Physics*. Academic Press.
Hobiger, M. & Fäh, D., 2020. Site characterization report SEFS: erstfeld (UR) - Schule, Available at: https://stations.seismo.ethz.ch/static/sitecharacterization/filearchive/project/Site_Characterization/Array/SEFS_00/DOC/analysis/SEFS-Report.pdf, last accessed July 2022
Khanbabazadeh, H., Hasal, M.E. & Iyisan, R., 2019. 2D seismic response of the Duzce Basin, Turkey, *Soil Dyn. Earthq. Eng.,* **125,**.
Kramer, R., Lu, Y. & Bokelmann, G., 2023. Interaction of air pressure and groundwater as main cause of sub-daily relative seismic velocity changes, *Geophys. Res. Lett.,* **50**(7), e2022GL101298, doi:10.1029/2022GL101298.
Le Roux, O., Cornou, C., Jongmans, D. & Schwartz, S., 2012. 1-D and 2-D resonances in an Alpine valley identified from ambient noise measurements and 3-D modelling, *Geophys. J. Int.,* **191,** 579–590.
Lebrun, B., Hatzfeld, D. & Bard, P. Y., 2002. Site effect study in urban area: experimental results in Grenoble (France), in *Earthquake Microzoning,* pp. 2543–2557, Birkhäuser.
Longuet-Higgins, M.S., 1950. A theory of the origin of microseisms, *Phil. Trans. R. Soci. Lond., A,* **243**(857), 1–35.
MONITRON, A.G., 2018. Hydrografiches jahrburch '17, Available at: https://www.ur.ch/_docn/189377/Hydrografisches_Jahrbuch_2017_komplett_ohne_Karten.pdf, last accessed July 2022.
Peterson, J., 1993. Observations and modeling of seismic background noise, USGS Open-File Report 93-322.
Ramírez, J.A., Boroschek, R.L., Aguilar, R. & Ventura, C.E., 2022. Daily and seasonal effects of environmental temperature and humidity on the modal properties of structures, *Bull. Earthq. Eng.,* **20,** 4533–4559.
Richter, T., Sens-Schönfelder, C., Kind, R. & Asch, G., 2014. Comprehensive observation and modeling of earthquake and temperature related seismic velocity changes in northern Chile with passive image interferometry, *J. geophys. Res.,* **119,** 4747–4765.
Ringler, A.T. *et al.*, 2021. A review of timing accuracy across the Global Seismographic Network, *Seismol. Res. Lett.,* **92**(4), 2270–2281.
Ringler, A.T., Evans, J.R. & Hutt, C.R., 2015. Self-noise models of five commercial strong-motion accelerometers, *Seismol. Res. Lett.,* **86**(4), 1143–1147.
Roeloffs, E.A., 1988. Fault stability changes induced beneath a reservoir with cyclic variations in water level. *J. geophys. Res.,* **93**(B3), 2107–2124.
Roten, D., Fäh, D., Cornou, C. & Giardini, C., 2006. Two-dimensional resonances in Alpine valleys identified from ambient vibration wavefields, *Geophys. J. Int.,* **165,** 889–905.
Saul, M.J. & Lumley, D.E. 2013. A new velocity–pressure–compaction model for uncemented sediments, *Geophysical Journal International,* **193**(), 905–913.
Sgattoni, G. & Castellaro, S., 2020. Detecting 1D and 2D ground resonances with a single-station approach, *Geophys. J. Int.,* **223,** 471–487.
Suzuki, Y., Iiyama, K., Morikawa, H., Sakai, K. & Araki, G., 2021. New method to estimate bedrock shape of small-scale basin using modal properties of sediments, *Soil Dyn. Earthq. Eng.,* **149,** doi:10.1016/j.soildyn.2021.106882.
Terzaghi, K., 1923. Die berechnug der durchlassigkeit des tones aus dem verlauf der hydromechanischen Spannungserscheinungen, *Sitzungsber. Akad. Wiss. (Wien), Math. - Naturwiss. Kl., Abt. Iia,* **132,** 125–138.
Vassallo, M., Cultrera, G., Di Giulio, G., Cara, F. & Milana, G., 2022a. Peak frequency changes from HV spectral ratios in Central Italy: effects of strong motions and seasonality over 12 years of observations, *J. geophys. Res.,* **127**(5), e2021JB023848,.
Vassallo, M., Riccio, G., Mercuri, A., Cultrera, G. & G., 2022b. H/V noise and earthquake automatic analysis (HVNEA), *Seismol. Soc. Am.,* **94**(1), 350–368.
Xiao, W. & Wang, Y., 2022. Characteristics of horizontal to vertical spectral ratio of InSight seismic data from Mars, *J. geophys. Res.,* **127**(6), e2020JE006813, doi:10.1029/2020JE006813.

APPENDIX

We present the modal amplitudes and damping trends over time, for the same seismic stations (SEFS, SIOO, OGFO, GARG and BOSI) discussed in the main text.

Time stability of modal amplitudes

Microtremor amplitude depends on several ambient sources and inevitably changes over time. At frequencies below 1 Hz, as those discussed in the paper, the noise sources are dominantly meteorological, oceanic and atmospheric perturbations. It is typical to see the 0.17 Hz (Longuet-Higgins 1950) peak in the winter spectra, disappearing in calm days. Spectral peaks of stratigraphic origin (resonances) can be distinguished from meteorological/oceanic peaks because they remain stable over time, at least within the seasonal variability discussed in the main text.

In Fig. 11, we show an example of spectra recorded at GARG and OGFO in a calm day (25/05/2021 and 27/04/2017) and in a foul day (30/12/2021 and 12/01/2017). The peaks of stratigraphic origin can always be seen, while the 0.17 Hz ocean peak vanishes in calm days.

The remarkable correlation of the modal spectral amplitudes with wintertime is illustrated in Fig. 12. L1 amplitudes are greater than T1, which are greater than the vertical and higher modes. The amplitude of motion at the resonance frequencies decreases between 70 and 90 per cent in summer compared to winter.

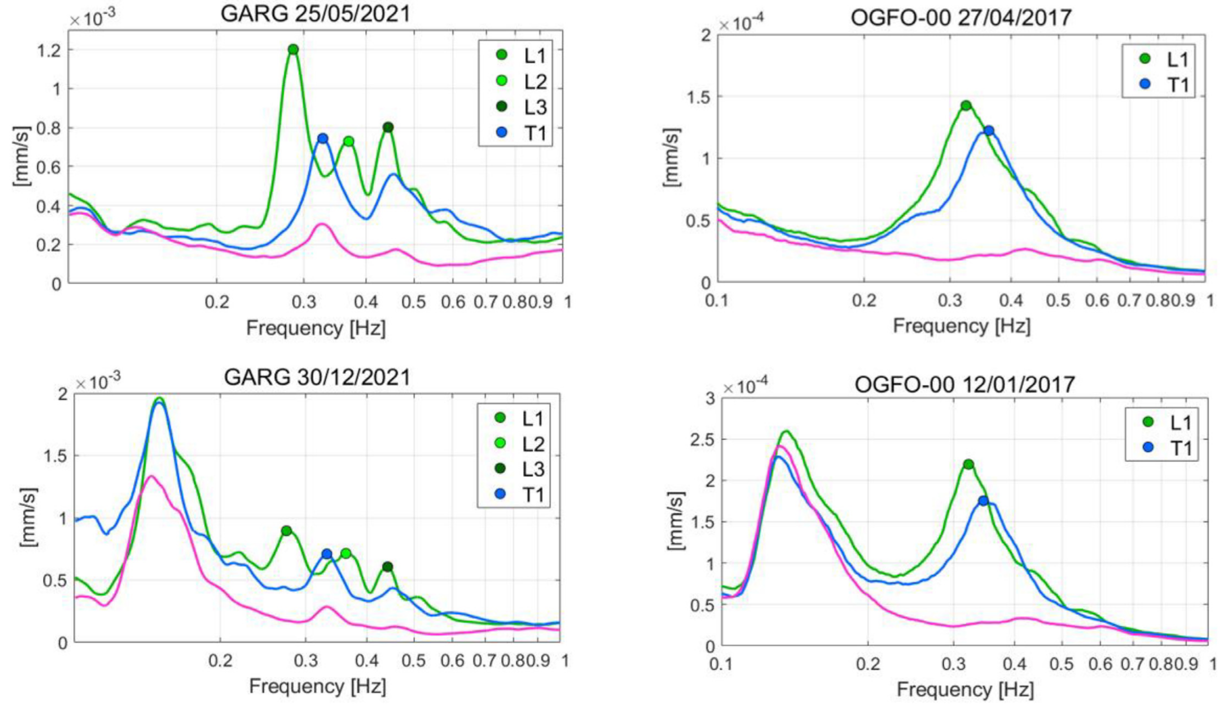

Figure 11. Average spectral components of motion (green: longitudinal, blue: transversal, magenta: vertical) under different ambient excitation conditions at GARG and OGFO. The main identified eigenfrequencies of the basins are marked by the dots. The 0.17 Hz peaks in the bottom panels are of oceanic origin.

Time stability of modal damping

To conclude the time-dependent dynamic characterization of the case studies, in Fig. 13 we present the modal damping computation as in Chopra (1995).

When it can be seen (SEFS and SIOO), we observe a larger damping in summertime compared to winter time. In other words, the modal frequency summer increase is accompanied by a modal damping decrease, which is not as one would expect from the elasticity theory.

It is to be noted that the computation of damping from ambient noise data can be affected by some uncertainty (Castellaro 2016a).

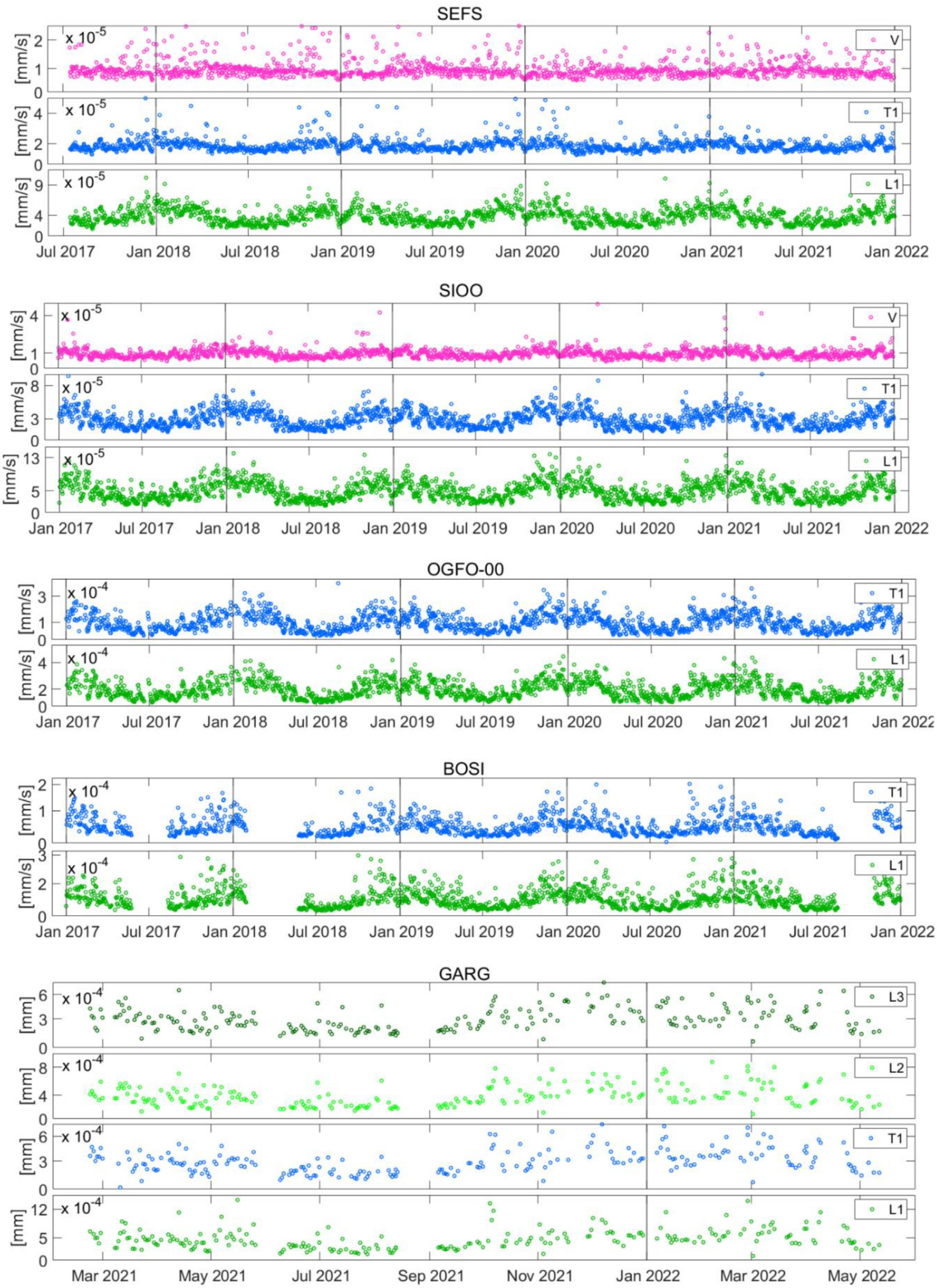

Figure 12. Eigenfrequency amplitudes identified at the inspected sites in the time interval analysed. Longitudinal modes are in green, transversal modes in blue and vertical modes in magenta.

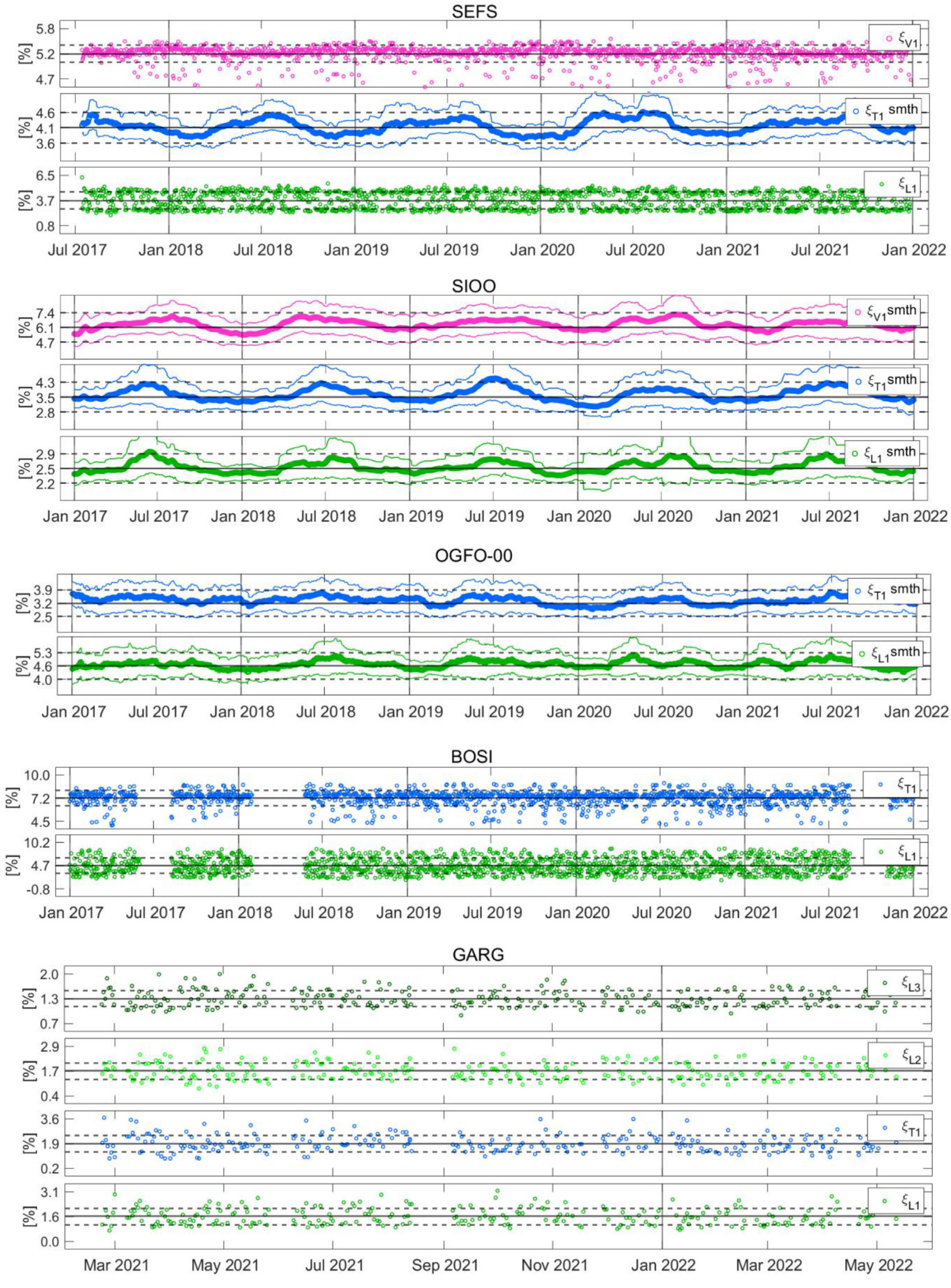

Figure 13. Modal damping dependence with time at the selected stations.